ORNL/CP-99115

CONF-980921--

HYDROGEN RETENTION IN ION IRRADIATED STEELS

John D. Hunn
Oak Ridge National Laboratory
P.O. Box 2008
Oak Ridge, Tennessee 37831-6376
(423) 574-2480

M.B. Lewis
Oak Ridge National Laboratory
P.O. Box 2008
Oak Ridge, Tennessee 37831-6376
(423) 574-5054

E.H. Lee
Oak Ridge National Laboratory
P.O. Box 2008
Oak Ridge, Tennessee 37831-6376
(423) 574-5058

ABSTRACT

In the future 1-5 MW Spallation Neutron Source, target radiation damage will be accompanied by high levels of hydrogen and helium transmutation products (500-1000 appm H/dpa and 50-200 appm He/dpa). Helium is known to be trapped in steels in the form of gas bubbles which contribute to hardening. There is evidence that hydrogen also can be trapped in steels and contribute to further hardening. We have recently carried out investigations using simultaneous Fe/He/H multiple-ion implantations into 316LN stainless steel between 50 and 350°C to simulate the type of radiation damage expected in spallation neutron sources. Hydrogen and helium were injected at appropriate energy and rate, while displacement damage was introduced by nuclear stopping of 3.5 MeV Fe^+, 1 μm below the surface. Nano-indentation measurements showed a cumulative increase in hardness as a result of hydrogen and helium injection over and above the hardness increase due to the displacement damage alone. TEM investigation indicated the presence of small bubbles of the injected gases in the irradiated area.

In the current experiment, the retention of hydrogen in irradiated steel was studied in order to better understand its contribution to the observed hardening. To achieve this, the deuterium isotope (^2H) was injected in place of natural hydrogen (^1H) during the implantation. Trapped deuterium was then profiled, at room temperature, using the high cross-section nuclear resonance reaction with ^3He. Results showed a suprisingly high concentration of deuterium to be retained in the irradiated steel at low temperature, especially in the presence of helium. There is indication that hydrogen retention at spallation neutron source relevant target temperatures may reach as high as 10%.

I. INTRODUCTION

In the design of an accelerator-based 1-5 MW spallation neutron source (SNS),[1] materials performance in the irradiated target vessel is of paramount importance. Displacement rates up to 10^{-2} dpa/s are expected during the 1 μs, 30-60 Hz pulse. These will be accompanied by the formation of numerous neutron induced transmutation products, the most prevalent being hydrogen and helium with production rates as high as 1000 appm H/dpa and 200 appm He/dpa. The temperature of the stainless steel target vessel is expected to be between 80 and 130°C and no higher than 200°C. In a previous paper[2] we reported on nanohardness and microstructural changes in a 316LN alloy which had been irradiated with 3.5 MeV ^{56}Fe in order to introduce 50 dpa peak displacement damage during simultaneous injection of hydrogen and helium with 180 keV $^1H^+$ and 360 keV $^4He^+$ beams. Figure 1 summarizes the results of the nanohardness tests for different beam combinations and target temperatures.

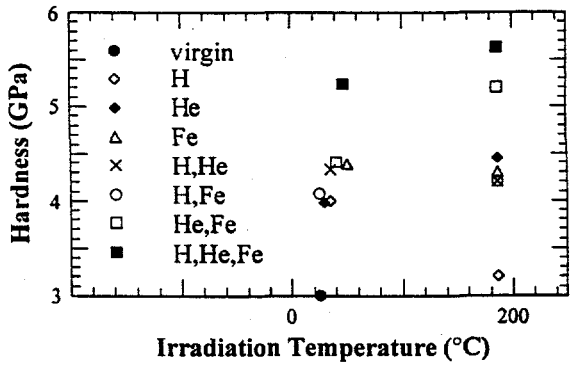

Figure 1 : Nanohardness at 200 nm depth (see reference [2] for irradiation conditions).

DISCLAIMER

DISCLAIMER

Portions of this document may be illegible in electronic image products. Images are produced from the best available original document.

The hardening from iron is expected to be due to accumulation of displacement damage. The peak displacement damage introduced by the deuterium and helium is a small fraction of that from iron (0.8 dpa each). Even so, the observed hardening from single ion irradiations with these two ions could still be due to displacement damage. Hardening has been observed in neutron irradiated austenitics at doses as low as 10^{-3} dpa[3,4] Dose dependence measurements on our triple-beam irradiations show onset of hardening at 0.1 dpa with no increase in hardening from 1 to 40 dpa. Displacement damage alone, however, does not explain the increased hardening observed in the high dose multiple beam irradiations where the additional H and He dpa are negligible when added to the 50 dpa from Fe.

When helium is implanted into steel, it rapidly diffuses as an interstitial but over a very short diffusion length before being trapped by a vacancy, effectively resulting in negligible migration from the implantation site.[5,6] The trapped helium is known to cluster into small bubbles which also contributes to hardening.[6,7] The question arises as to whether hydrogen might also be trapped as bubbles and produce hardening. This is of critical importance in the SNS environment, where H production will be five times higher than He. In order to better understand the role of hydrogen in the irradiation hardening, the hydrogen retention has been studied. It was possible to profile the hydrogen by substituting the deuterium isotope during the irradiation and using a nuclear reaction analysis technique as described in the next section.

Hydrogen is generally considered to be a fast diffuser in steel at these temperatures. Previous studies, however, have found that hydrogen can be trapped at moderate temperatures in the presence of radiation damage and/or helium bubbles and defect trapping of hydrogen and helium in metals has been studied in depth.[8-14] Most of these previous experiments involved shallow, low energy implantation (≤10 keV). Although this aids in the analysis, higher implantation energies were chosen in the present work in order to avoid surface effects in the development of the irradiation microstructure. In addition, this work differs by simultaneously injecting hydrogen and helium as opposed to sequential implantation.

II. EXPERIMENTAL PROCEDURES

The sample material was nuclear quality 316LN stainless steel, heat #18474 from Jessop Steel Company. Chemical analysis verified the material to meet AISI specifications for 316LN steel and SEM analysis showed a clean grain structure with very little slag or precipitates. Thin 10 mm square wafers were cut from a 25 mm cold-rolled slab and ground flat with 600, 800, and 1200 grit polishing paper to a final thickness between 0.4 and 0.8 mm. Wafers were then solution annealed at 1050°C for 2 hours in a good vacuum ($<2\cdot10^{4}$ Pa) to remove cold working introduced by the grinding step. The resulting grain structure was fairly uniform with an average grain size of 0.1 mm. Deep channels along the grain boundaries could be observed suggesting that some thermal etching occurred. Samples were electropolished in a perchloric/acetic acid solution to remove these channels and expose pristine material. Some pitting was introduced by the electropolish due to the difficulty in uniformly polishing such large specimens.

Implantations were performed at the Oak Ridge National Laboratory (ORNL) Triple Ion-beam Facility (TIF).[15] The TIF can provide simultaneous ion beams from up to three separate Van de Graaff accelerators. The deuterium beam was normal to the target, the helium and iron beams came in at 15° off normal. The beam current and uniformity over a 10 mm square area were periodically monitored by an array of miniature faraday cups integrated to a continuously monitoring profilometer in order to calculate the accumulated fluence for each of the ion beams. Samples were mounted on copper blocks heated from the back with an electron gun and monitored internally by a type-K thermocouple. Internal block temperature varied from independently measured sample surface temperature by less than 5% during implantation. Pressure at the sample was less than 10^{-5} Pa.

Table 1 : Implantation parameters

Implanted Ion	Energy (keV)	Fluence (ions/m^2)	Relative Flux
^{56}Fe	3500	$5.0\cdot10^{20}$	1
^{2}H	150	$1.3\cdot10^{21}$	2.6
^{4}He	360	$3.0\cdot10^{20}$	0.6

The appropriate energy and fluence for each ion were chosen using SRIM-98 with the modified Kinchin-Pease approximation.[16] The number of displacements per atom (dpa) was calculated using the NRT formula[17]

$$\text{dpa} = \frac{.8T_{dam}}{2E_d} \cdot \frac{\text{ion fluence}}{\text{target density}}, \qquad (1)$$

where T_{dam} is the sum of all nuclear energy losses from SRIM in eV/ion/m and E_d (40 eV for steel) is the displacement energy. Table 1 lists the calculated implantation parameters to achieve an average of 50 dpa at 0.8 μm with relative average H and He injection ratios of

1000 appm H/dpa and 200 appm He/dpa. These conditions were chosen to duplicate the previous experiment shown in figure 1, with ^{2}H substituted for ^{1}H. Averages were obtained by calculating the mean within plus or minus one half width of the gaussian peak. The time for each implantation was about 5 hours with the Fe flux varying between $2 \cdot 10^{16}$ to $3 \cdot 10^{16}$ ions/m^2/s and the relative flux ratios held constant. Figure 2 shows an overlay of the simulated profiles.

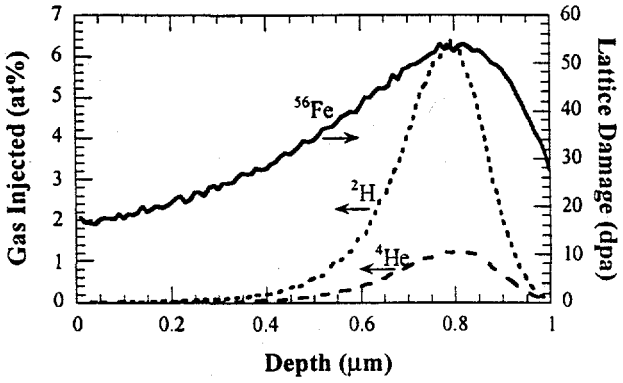

Figure 2 : SRIM simulation of implantation parameters

After implantation, samples were cooled to room temperature and the deuterium was profiled utilizing the nuclear reaction $^{2}H(^{3}He,^{1}H)^{4}He$ (Q=18.352 MeV). The nearly angular independent cross section for this reaction as a function of energy is shown in figure 3. In order to maximize the analysis sensitivity, a 1.4 MeV ^{3}He analyzing beam was chosen such that the energy of the ^{3}He at the expected deuterium peak concentration depth of 0.8 μm would be in the range of the broad resonance band in the cross section centered at 0.64 MeV.

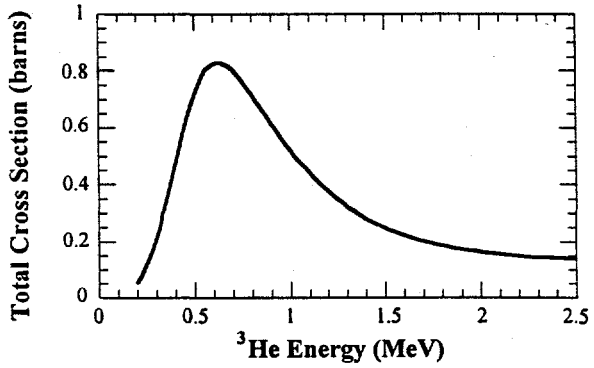

Figure 3 : Cross section for $^{2}H(^{3}He,^{1}H)^{4}He$.[18]

Protons between 12 to 14 MeV were detected by a 1500 μm thick silicon charged particle detector. The detected protons were counted and sorted as a function of energy by a multichannel analyzer. A 12.4 μm thick aluminized mylar stopping foil was placed in front of the detector to block the backscattered ^{3}He and ^{4}He. This reduces pulse pile-up in the detector and results in essentially zero background, allowing for very sensitive measurement. The detector was fixed at a scattering angle of 170° and presented a solid angle of 1 msr to the sample. Alpha particles from the equivalent reaction $^{2}H(^{3}He,^{4}He)^{1}H$ were simultaneously detected in a second 100 μm thick silicon detector with a 6.2 μm stopper foil which blocked the high flux of backscattered ^{3}He but let the ^{4}He and ^{1}H reaction products through. The high energy protons were not fully stopped in this thinner detector but, with a properly selected scattering angle, the partial energy proton peak could be separated from the alpha peak. However, due to increasing angular dispersion as a function of penetration depth of the incident ^{3}He ion, the depth resolution of the alpha spectrum was inferior to that of the proton spectra below 0.5 μm. Deuterium profiles discussed below were deconvoluted from the proton spectra only. Alpha spectra profiles were verified to be consistent with these higher resolution results.

A serious limitation to the NRA technique for deuterium profiling stems from the effect of the ^{3}He analysis beam on the deuterium profile.[19] In the present experiment, a measurable diffusion of deuterium was observed both as a function of flux and of fluence. The shape and net concentration of the deuterium profile could be seen to change with increasing fluence. This effect appeared to be magnified above a flux of $1 \cdot 10^{17}$ ions/m^2/s, probably due to excessive beam heating. Therefore, analysis was performed below this flux threshold. In order to maximize the resolution, spectra were accumulated to as high a fluence as possible with the stipulation that less than 5% reduction of the total concentration be observed and that the shape of the profile remain qualitatively unchanged. This was typically at a fluence of about $6 \cdot 10^{20}$ $^{3}He/m^2$. It should be noted that this fluence is twice that of the ^{4}He injected during the implantation step and might be expected to have greater than a 5% effect on the results. However, the range of 1.4 MeV ^{3}He is greater than 2 μm and very little is stopped in the first μm that is under study.

Deuterium concentration depth profiles were extracted from the raw proton yield versus energy spectra by a mathematical deconvolution technique.[20] This technique folds in the energy loss and dispersion of the incident ^{3}He and the exiting reaction product ^{1}H with the energy dependent cross section of the nuclear reaction. The yield Y in each multichannel analyzer bin of energy E_r and width ΔE_r can be written as a convolution integral of the deuterium density ρ, the reaction cross section σ, and the probability distribution functions P of the incident ion

and reaction product.

$$\frac{Y(E_r)}{\Delta(E_r)} = \iint \rho(x)P_i(E_i,x)\sigma(E_i)P_r(E_r,x)dE_i dx \quad . \qquad (2)$$

The probability functions take into account stopping, straggling, and multiple scattering in the target and stopper foils as well as scattering angle, detector resolution, and solid angle. With the appropriate approximations described in reference [20], equation (2) may be solved for the deuterium density function in such a form that can be computed by linear iteration.

A series of deuterated polystyrene standards were used to verify the nuclear analysis and deconvolution technique. Results agreed to within 10% of the reported deuterium concentration. Error bars shown in the deuterium density profiles below are calculated from the statistical resolution of the acquired raw spectra.

III. RESULTS AND DISCUSSION

Figure 4 summarizes the deuterium retention results for the 316LN wafers irradiated at several temperatures and different combinations of the ion beams listed in Table 1. The percent retention was calculated by integrating the area under the deconvoluted deuterium profile from 0.2 to 1.2 μm and dividing by the implanted fluence. The first 0.2 μm was excluded because of surface trapping discussed below. The maximum analysis depth of 1.2 μm corresponds to the depth where the 1.4 MeV ^{3}He analysis beam had slowed to 0.2 MeV, below which the reaction cross section is not well known. A higher energy ^{3}He beam can be used to increase the analysis depth but this was not necessary and would reduce the sensitivity in the area of interest as discussed in section II.

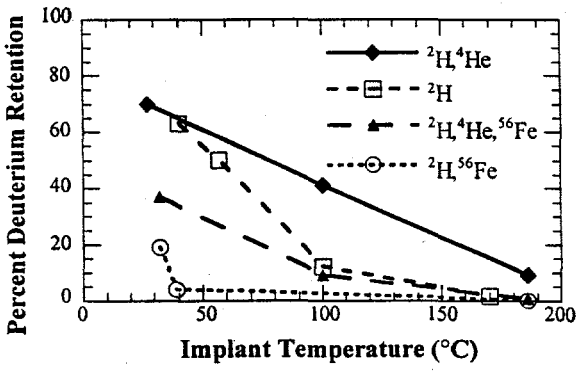

Figure 4 : Summary of deuterium retention (lines are to guide the eye).

Deuterium only implantation showed suprisingly high deuterium retention near room temperature. Greater than 40-60% retention below 50°C (still 2-3 times the helium injection concentration) probably explains why we observed similar hardening in figure 1 for the low temperature H and He implants. At higher temperature, where hydrogen retention was minimal, little hardening was observed. This suggests that in the H only implants, displacement damage alone did not produce the observed hardening. The displacement dose of 0.8 dpa, produced by the H irradiation, may not be sufficient to lead to hardening, even though, as discussed in section I, this was sufficient to result in hardening for the Fe irradiation. The difference in the primary knock-on atom (pka) spectra of H and Fe results in a different defect structure. The harder (denser) pka spectrum for Fe is expected to lead to the formation of defect clusters directly in the cascade. At a sufficient size and density, these clusters contribute to hardening. The softer H pka spectrum is expected to create mainly isolated point defects. TEM of the hydrogen only implant showed a high density of small black dots but no large dislocation loops.[2]

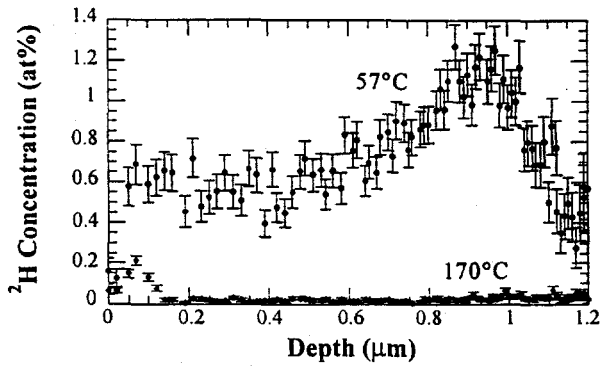

Figure 5 : Deuterium profile for ^{2}H implanted at 57 and 170°C.

Figure 5 shows profiles for 57 and 170°C irradiation temperature. At lower temperature, a peak at the average implantation depth can be seen as well as a considerable amount at shallower depths. This deuterium appeared to be weakly trapped. Several days at room temperature did not affect the profile. However, the deuterium profile was observed to readily change when irradiated by the ^{3}He analysis beam, with deuterium diffusing from the peak in both directions. Some of the deuterium that diffused toward the surface was trapped there, forming a surface peak similar to that shown in figure 5 for the 170°C implant. This may be due to trapping by near surface defects or may be due to a surface oxide. Previous thermal desorption studies of 5 keV ^{2}H-implanted steel have shown a strong desorption stage at 90°C, thought to be

caused by release from sub-surface vacancies.[14] During irradiation at 170°C, deuterium was apparently thermally detrapped and diffused away from the weak traps, which were sufficient to retain the deuterium at lower temperature.

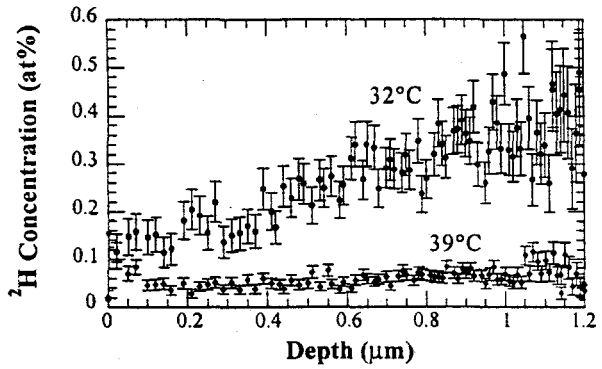

Figure 6 : Deuterium profile for (^{2}H, ^{56}Fe) dual-irradiation at 32 and 39°C.

Co-implantation of ^{56}Fe and ^{2}H resulted in a dramatic reduction in the retained deuterium as well as an apparent shift to lower temperature for thermal detrapping (figure 4, compare open circles to open squares). In figure 6, no end of ^{2}H range peak is evident, and at 39°C almost all of the deuterium has diffused away from the implanted layer. The effect of ion-irradiation-induced diffusion has been discussed by Myers.[19] Mechanisms include cascade mixing, enhanced diffusion by mobile point defects, rapid diffusion along extended defects, and trapping by irradiation defects. All except the last mechanism act to increase diffusion. As discussed above, we observed deuterium migration induced by the ^{3}He analysis beam. This effect was much greater for the more massive ^{56}Fe ion where the cascade volume, vacancy production, and defect density were greater.

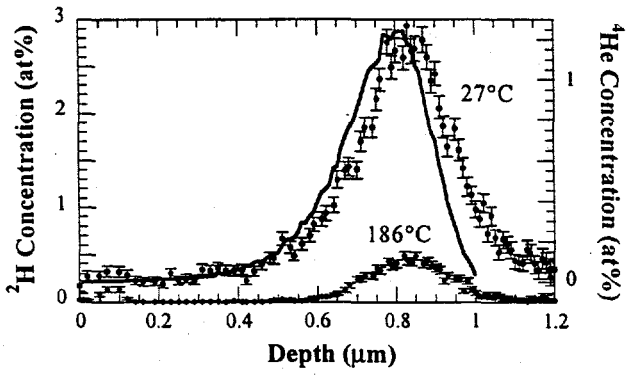

Figure 7 : Deuterium profile for (^{2}H, ^{4}He) dual-irradiation at 27 and 186°C compared to SRIM simulated ^{4}He profile (solid line).

In contrast, co-implantation of ^{4}He and ^{2}H showed the opposite effect on the deuterium retention. Deuterium concentrations for higher temperature irradiations were significantly greater than for ^{2}H implantation alone, with 9% retention even at 186°C. In addition the trap strength appeared to be greater for these samples. Detrapping as a function of fluence during analysis by the ^{3}He beam was significantly less, suggesting a different trapping mechanism. Hydrogen trapping in metals pre-implanted with helium has been previously observed and identified as trapping by helium bubbles.[10,13] Figure 7 shows a deuterium density profile for the 27°C implant that is more well defined than in figure 5. This profile closely replicates the shape of the implanted ^{4}He profile simulated by SRIM, supporting the hypothesis that deuterium is trapped by the immobile helium. The slight offset in position may be due to the energy calibration used in the deconvolution or may represent a real discrepancy between the simulated and actual ^{4}He ion range. The fact that deuterium is still retained at 186°C, in the presence of helium, illustrates the relative strength of this trapping mechanism compared to that for ^{2}H-irradiation alone, where less than 1% is retained at this temperature.

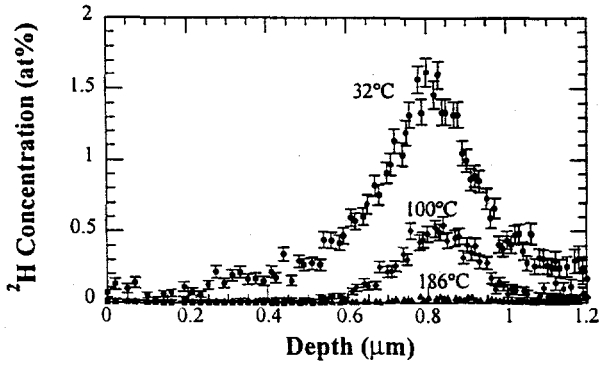

Figure 8 : Deuterium profile for (^{2}H, ^{4}He, ^{56}Fe) triple-irradiation at 32, 100, and 186°C.

Triple-ion-beam irradiations showed a combination of the enhanced retention by trapping at the helium bubbles and the enhanced diffusion due to the Fe-beam. Deuterium concentrations were lower than for (^{2}H, ^{4}He) dual-beam irradiations but still exhibited profiles which replicated the implanted helium profile (figure 8). Deuterium retention at room temperature was almost 40% (twice the concentration of injected helium). This might explain the increased hardening shown in figure 1 for the triple-beam irradiation at low temperature. Figure 1 also shows there was increased hardening for the triple-ion implanted sample at higher temperature. However, at this temperature, less than 1% deuterium retention was measured. This is negligible when added to the amount of

helium implanted. This suggests that the large amount of implanted hydrogen exerts some effect on the hardening even when it is not retained.

IV. CONCLUSIONS

Single-, dual-, and triple-ion-beam irradiations of 316LN stainless steel were performed at hydrogen and helium gas injection to dpa ratios relevant to spallation conditions. Deuterium retention was analyzed in order to better understand its contribution to irradiation-induced hardening. At an irradiation temperature of 100°C (in the range of the expected target vessel temperature of the SNS), 10% deuterium retention was observed for a sample irradiated to 50 dpa, 50,000 appm H, and 10,000 appm He. Deuterium was found to be strongly trapped in the presence of helium bubbles, with as high as 70% retention at room temperature. Samples implanted with deuterium alone were observed to retain over 60% of the injected amount at room temperature and greater than 10% at 100°C. The effect of the iron implantation, used to produce displacement damage, was to increase the out-diffusion of the injected deuterium. In the SNS, where displacement damage will be primarily generated by GeV protons and spallation spectrum neutrons, this enhanced diffusion effect may differ due to second order effects such as displacement rate and pka spectrum.

ACKNOWLEDGEMENTS

Research sponsored by the Division of Materials Sciences, U.S. Department of Energy under contract number DE-AC05-96OR22464 with Lockheed-Martin Energy Research Corporation.

REFERENCES

1. *National Spallation Neutron Source Conceptual Design Report*, NSNS/CDR-2/V1 and V2, Oak Ridge National Laboratory, U.S. Department of Energy, May 1997.

2. E.H. Lee, G.R. Rao, J.D. Hunn, P.M. Rice, M.B. Lewis, S.W. Cook, K. Farrell, and L.K. Mansur, "Triple ion-beam studies of radiation damage effects in a 316LN austenitic alloy for a high power spallation neutron source." *Materials for Spallation Neutron Sources* edited by M.S. Wechsler, L.K. Mansur, C.L. Snead, and W.F. Sommer, pp. 57-65, The Minerals, Metals and Materials Society, Warrendale (1998).

3. H.R. Higgy and F.H. Hammad, "Effect of Fast-Neutron Irradiation on Mechanical Properties of Stainless Steels: AISI types 304, 316, and 347," *J. of Nucl. Mater.* **55**, 177-186 (1975).

4. K. Farrell and S.T. Mahmood, unpublished.

5. M. B. Lewis and K. Farrell, "Migration Behavior of Helium Under Displacive Irradiation in Stainless Steel, Nickel, Iron, and Zirconium," *Nucl. Instr. and Meth.* **B16**, 163-170 (1986).

6. L.K. Mansur, E.H. Lee, P.J. Maziasz, and A.F. Rowcliffe, "Control of Helium Effects in Irradiated Materials Based on Theory and Experiment," *J. of Nucl. Mater.* **141-143**, 633-646 (1986).

7. M.B. Toloczko, G.E. Lucas, G.R. Odette, R.E. Stoller, and M.L. Hamilton, "An Investigation of Microstructures and Yield Strengths in Irradiated Austenitic Stainless Steels Using Small Specimen Techniques", *Effects of Radiation on Materials, 17th Int. Symp. ASTM STP 1270*, edited by D.S. Gelles, R.K. Nanstad, A.S. Kumar, and E.A. Little, pp. 902-918, American Society for Testing and Materials, Ann Arbor (1996).

8. M.B. Lewis and K. Farrell, "Nuclear Microanalysis as a Probe of Impurity-Defect Interactions," *Advanced Techniques for Characterizing Microstructures*, edited by F.W. Wiffen and J.A. Spitznagel, pp. 487-501, Metallurgical Society of AIME (1982).

9. S.T. Picraux, "Defect Trapping of Gas Atoms in Metals," *Nucl. Instr. and Meth.* **182/183**, 413-437 (1981).

10. F. Besenbacher , J. Bøttiger, and S.M. Myers, "Deuterium Trapping in Helium-Implanted Nickel," *J. Appl. Phys.* **53**, 3547-3551 (1982).

11. W. Möller, "The Behavior of Hydrogen Atoms Implanted into Metals," *Nucl. Instr. and Meth.* **209/210**, 773-790 (1983).

12. F. Besenbacher, S.M. Myers, and J.K. Nørskov, "Interaction of Hydrogen with Defects in Metals," ," *Nucl. Instr. and Meth.* **B7/8**, 55-66 (1985).

13. M. Ogawa, K. Saneyoshi, Y. Takagi, A. Shirota, and Y. Suzawa, "Critical Helium Fluence for Hydrogen Trapping in Pre-Damaged Stainless Steel," *J. of Nucl. Mater.* **149**, 247-251 (1987).

14. N. Yoshida, N. Ashizuka, T. Fujiwara, T. Kurita, and T. Muroga, "Radiation Damage and Deuterium Trapping in Deuterium Ion Irradiated Austenitic Stainless Steel," *J. of Nucl. Mater.* **155-157**, 775-780 (1988).

15. M.B. Lewis, W.R. Allen. R.A. Buhl, N.H. Packan, S.W. Cook, and L.K. Mansur, "Triple Ion Beam

Irradiation Facility," *Nucl. Instr. and Meth.* **B43**, 243-253 (1989).

16. J.F. Ziegler, J.P. Biersack, and U. Littmark, *Stopping and Ranges of Ions in Matter*, Pergamon Press, New York (1985).

17. M.J. Norgett, M.T. Robinson, and I.M. Torrens, "A Proposed Method of Calculating Displacement Dose Rates," *Nucl. Eng. Des.* **33**, 50-54 (1975).

18. W. Möller and F. Besenbacher, "A Note on the 3He+D Nuclear-Reaction Cross Section," *Nucl. Instr. and Meth.* **168**, 111-114 (1980).

19. S.M. Myers, "Ion-Beam-Induced Migration and Its Effect on Concentration Profiles," *Nucl. Instr. and Meth.* **168**, 265-274 (1980).

20. M.B. Lewis, "A Deconvolution Technique for Depth Profiling with Nuclear Microanalysis," *Nucl. Instr. and Meth.* **190**, 605-611 (1981).